# Effect of Chalcogen Atom Substitution on the Optoelectronic Properties in Cyclopentadithiophene Polymers

Miquel Planells,* Bob C. Schroeder, and Iain McCulloch

Department of Chemistry, Imperial College London, London SW7 2AZ, U.K.

S Supporting Information

ABSTRACT: We report the synthesis and characterization of a series of cyclopentadithiophene polymers containing thiophene, selenophene, and tellurophene as comonomers. The effect of the chalcogen atom has been studied by a range of techniques, including thermal, optical, electrochemical, and computational. The results showed that by increasing the size of the chalcogen atom, the optical band gap is reduced mainly due to a downshift in the LUMO energy level. In addition, the larger size also increases the intermolecular heteroatom–heteroatom interactions facilitating the formation of polymer aggregates. This led to not only a stronger red-shifted band in the UV–vis absorption spectrum as well as raise in the HOMO energy level but also a potential solubility issue for higher molecular weight polymers containing particularly tellurophene units.
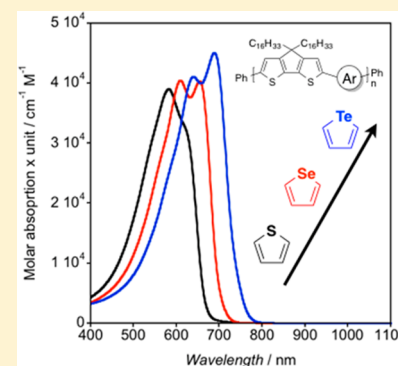
1. INTRODUCTION

Semiconducting materials have been attracting interest from both an academic and commercial perspective due to their potential high-performance/low-cost proposition as well as solution processability for organic electronic devices. Proposed applications may include but not limited to solar cells,[1,2] light-emitting diodes,[3] field effect transistors,[4,5] bioelectronics,[6] sensors,[7] nonlinear optics,[8] and spintronics.[9]

This synthetic versatility underpins a facile molecular design optimization or so-called "chemical engineering" which can be carried out by attaching a wide range of electron donor and/or acceptor groups, solubilizing entities on the peripheral positions, or even fusing units, leading to an incredible fine-tuning not only on the optical and electronic properties but also on the solid state packing.[10] Another interesting approach to finely tune the material properties is to replace the sulfur atom by a different chalcogen atom, such as selenium and tellurium, resulting in five-member ring heteroaromatic equivalent of thiophene. Interestingly, the incorporation of these larger and heavier heteroatoms makes selenophene and tellurophene units more electron donating and polarizable than the thiophene counterpart.[11] This property has an important effect on the chemical reactivity, where selenophene and tellurophene are more reactive versus electrophilic aromatic substitutions compared to thiophene as its aromaticity decreases.[11] Furthermore, the chalcogen atom has an impact on the optical properties by reducing the band gap as its size increases, by upraising the HOMO and lowering the LUMO energy levels.[12] Despite having this outstanding versatility by only one atom substitution, less attention has been focused on selenophene and especially tellurophene derivatives, probably due to the higher toxicity and less commercial availability of Se and Te precursors.[11] Moreover, most of the work has been

carried out on discrete molecules,[13,14] and only a few examples of polymers incorporating selenophene and tellurophene can be found in the literature.[15–20] The addition of heavier atoms is believed to lead to a systematic increase of the spin–orbit coupling,[21] and therefore chalcogenophene-containing polymers would be interesting to explore in the spintronics area.[22]

Among all available conjugated repeat units, thiophenes have been extensively used in semiconducting polymers due to their high polarizability, effective electronic conjugation, chemical stability, and astonishing synthetic versatility.[23]

Herein, we describe the synthesis and characterization of three cyclopentadithiophene (CPDT) based polymers with hexadecyl alkyl chain in order to ensure solubility. They are copolymerized with thiophene, selenophene, and tellurophene and have been studied using thermal, optical, electrochemical, and computational means. The polymer chemical and physical properties were discussed and correlated with the heteroatom effect.

2. EXPERIMENTAL SECTION

2.1. Synthetic Procedure. *Materials.* All starting materials were reagent grade and purchased from commercial suppliers unless otherwise specified. Anhydrous solvents were bought from Acros Organics over molecular sieves (less than 0.01% H_2O).

Synthesis of 4,4-Dihexadecyl-4H-cyclopenta[2,1-b:3,4-b']-dithiophene (1). $4H$-Cyclopenta[2,1-b:3,4-b']dithiophene (1.78 g, 10 mmol) and NaOtBu (3.8 g, 40 mmol) were added in a round-bottom flask with 50 mL of dry DMSO. The mixture was heated at 50 °C, and 1-bromohexadecane (7.6 mL, 25 mmol) was added dropwise. The reaction was stirred at 50 °C overnight. The reaction mixture was

X = S; **C$_{16}$CPDT-T**
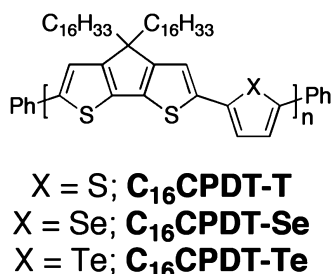X = Se; **C$_{16}$CPDT-Se**
X = Te; **C$_{16}$CPDT-Te**

Figure 1. Molecular structure of C$_{16}$CPDT based polymers used in this study.

quenched with water (400 mL) and extracted with Et$_2$O (400 mL). The organic phase was washed with distilled water twice, dried over MgSO$_4$, and filtered off. The crude was purified by column chromatography (SiO$_2$, hexanes) to afford the pure product as colorless oil that slowly solidified (5.05 g, 81% yield). ^{1}H NMR (400 MHz, CDCl$_3$) δ_H: 7.14 (d, J = 4.8 Hz, 2H); 6.93 (d, J = 4.8 Hz, 2H); 1.81 (m, 4H); 1.25 (m, 52H); 0.93 (m, 4H); 0.88 (t, J = 6.7 Hz, 6H). ^{13}C NMR (100 MHz, CDCl$_3$) δ_C: 158.3; 136.6; 124.5; 121.8; 53.4; 37.8; 32.1; 30.2; 29.8 (×6); 29.7 (×2); 29.5 (×2); 24.7; 22.8; 14.3.

Synthesis of 2,6-Dibromo-4,4-dihexadecyl-4H-cyclopenta[2,1-b:3,4-b']dithiophene (2). 4,4-Dihexadecyl-4H-cyclopenta[2,1-b:3,4-b']dithiophene (1.25 g, 2 mmol) was added in a round-bottom flask with 20 mL of THF and cooled down to 0 °C. NBS (730 mg, 4.1 mmol) was added at 0 °C, and the mixture was stirred overnight at room temperature. The reaction mixture was quenched with water (200 mL) and extracted with Et$_2$O (200 mL). The organic phase was washed with brine, dried over MgSO$_4$, and filtered off. The crude was purified by column chromatography (SiO$_2$, hexanes) to afford the pure product as colorless oil and then slowly solidified into a white solid (1.22 g, 78% yield). ^{1}H NMR (400 MHz, CDCl$_3$) δ_H: 6.92 (s, 2H); 1.75 (m, 4H); 1.25 (m, 52H); 0.91 (m, 4H); 0.88 (t, J = 6.9 Hz, 6H). ^{13}C NMR (100 MHz, CDCl$_3$) δ_C: 156.1; 136.4; 124.7; 111.2; 55.2; 37.7; 32.1; 30.1; 29.8 (×6); 29.7 (×2); 29.5 (×2); 24.7; 22.8; 14.3.

General Polymer Synthesis and Purification. An oven-dried microwave vial was charged with 1 equiv of **2** (94.2 mg, 0.12 mmol) and 1 equiv of distannylated thiophene[24] (49.1 mg, 0.12 mmol) or selenophene[25] (54.8 mg, 0.12 mmol) or tellurophene[26] (60.6 mg, 0.12 mmol) together with Pd(PPh$_3$)$_4$ (5.5 mg, 4.8 μmol, 4 mol %). The vial was sealed, and dry *o*-xylene (0.6 mL) was added. The reaction mixture was degassed with argon for 30 min before being placed in the microwave reactor and subjected to the following heating conditions: 100 °C for 2 min, 120 °C for 2 min, 140 °C for 2 min, 160 °C for 5 min, 180 °C for 5 min, and 200 °C for 30 min. Once the reaction had cooled, end-capping trimethyl(phenyl)tin (2.1 μL, 0.012 mmol) was added and heated to 120 °C for 1 min, 140 °C for 1 min, and 160 °C for 3 min. The same process was repeated for bromobenzene (1.3 μL, 0.012 mmol). Once the reaction had cooled, polymer crude solution was precipitated by adding it dropwise into an acidic MeOH solution (containing 1% HCl) and stirred for 1−3 h until fine powder was obtained. The precipitated was filtered off into a cellulose thimble, and Soxhlet extractions in acetone (16 h), hexane (16 h), and chloroform (2 h) were carried out. The hexane and chloroform fractions were combined and treated with diethyldithiocarbamic acid diethylammonium salt and reprecipitated in MeOH. Preparative GPC in chlorobenzene at 80 °C was carried out, and the polymer was

fractionated by molecular weight (MW). Low MW fractions were discarded, and high MW fractions were joined; the solvent was removed and reprecipitated by adding into a stirring MeOH solution to afford C$_{16}$CPDT-T (52 mg, 61%), C$_{16}$CPDT-Se (56 mg, 62%), and C$_{16}$CPDT-Te (46 mg, 48%) as dark solids. The collected polymer was dried under high vacuum for 24 h before any characterization took place.

2.2. Methods. *Chemical Characterization.* ^{1}H and ^{13}C NMR spectra were recorded on a Bruker Advance 400 spectrometer (400 MHz for ^{1}H and 100 MHz for ^{13}C). The deuterated solvents are indicated; chemical shifts, δ, are given in ppm, referenced to TMS, standardized by the solvent residual signal (^{1}H, ^{13}C). Number-average (M_n) and weight-average (M_w) molecular weights were determined with an Agilent Technologies 1200 series GPC in chlorobenzene at 80 °C, using two PL mixed B columns in series, and calibrated against narrow polydispersity polystyrene standards. DSC experiments were carried out with a TA Instruments DSC Q20, and TGA plots were obtained with a PerkinElmer Pyris 1 TGA.

Optical Characterization. Solution and solid state UV−vis absorption spectra were recorded using a UV-1601 Shimadzu UV−vis spectrophotometer.

Electrochemical Characterization. All cyclic voltammetry measurements were carried out in dry acetonitrile using 0.1 M [TBA][PF$_6$] electrolyte in a three-electrode system, with each solution being purged with N$_2$ prior to measurement. The working electrode was ITO-treated glass, the reference electrode was Ag/AgCl, and the counter electrode was a Pt rod. All cyclic voltammetry (CV) were made at room temperature using an AUTOLAB PGSTAT101 potentiostat at 50 mV/s scan rate and referenced to ferrocene.

Computational Details. The molecular structures were optimized in a vacuum without any symmetry constraints. All calculations were carried out using the Gaussian 09 program[27] with the Becke three-parameter hybrid exchange, Lee−Yang−Parr correlation functional (B3LYP) level of theory together with 6-311G(d) basis set for C, H, and S atoms. Se and Te atoms were treated with the SDD valence basis set and effective core potential.[28] All structures were input and processed through the Avogadro software package.[29] Time-dependent calculations (TD-DFT)[30,31] were performed using the same functional and basis set. The 10 lowest singlet electronic transitions were calculated and processed with GaussSum software package.[32]

3. RESULTS AND DISCUSSION

3.1. Synthesis and Chemical Properties. The synthesis of C$_{16}$CPDT based polymers is shown in Scheme 1. Hexadecyl (C$_{16}$) alkyl chains were chosen to ensure solubility throughout polymerization, in order to achieve as high molecular weight as possible, as well as to ensure processability of the polymers for subsequent thin film studies. Dibrominated C$_{16}$CPDT species **2** has been obtained by alkylation and subsequent bromination of plain CPDT following a modified reported procedure.[33] Distannylated thiophene,[24] selenophene,[25] and tellurophene[26] were used to copolymerize **2**, and polymers were attained via Stille coupling assisted by microwave irradiation and end-capped by phenyl groups.[34] Purification of the crude polymers was carried out by Soxhlet extraction with acetone, hexane, and then chloroform to extract the polymer product. Remaining palladium residues were extracted by treating the chloroform

Scheme 1. Synthesis of C$_{16}$CPDT Based Polymers
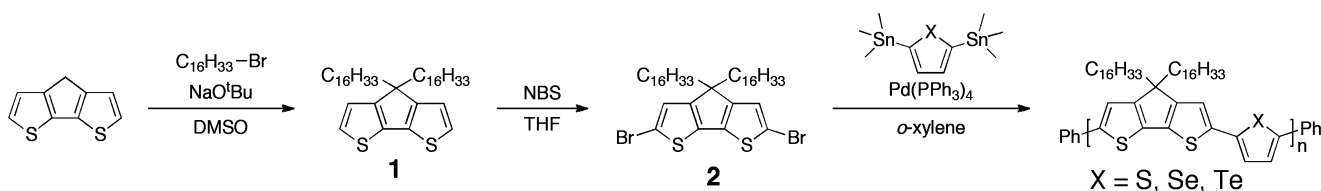
fraction with diethyldithiocarbamic acid diethylammonium salt. Finally, preparative GPC in chlorobenzene was also carried out in order to further purify our polymers and withdraw the very low molecular weight fraction that were not removed during Soxhlet extractions.[35]

Polymer molecular weights and polydispersity were determined by GPC analysis and referenced to polystyrene standards and are shown in Table 1. All three polymers show

Table 1. Polymer Chemical[a] and Thermal[b] Properties

polymer	M_n (g mol^{-1})	M_w (g mol^{-1})	PDI	DP_n^c	T_d (°C)
C_{16}CPDT-T	16000	32000	2.02	23	425
C_{16}CPDT-Se	24000	55000	2.35	32	414
C_{16}CPDT-Te	18000	37000	2.05	22	419

[a]Average molecular weight in number (M_n), in weight (M_w), and weight-average polydispersity PDI (M_w/M_n) as determined by GPC in chlorobenzene at 80 °C and calibrated on polystyrene standards. [b]Decomposition temperature determined by TGA under N_2 and based on 5% weight loss. [c]The degree of polymerization (DP_n) is defined in this case as the number of repeating units and calculated from GPC measurements.

very similar PDIs (~2) and similar molecular weights (~16K to 24K). Although difference in MW might slightly affect the polymer optoelectronic properties,[36] this series is suitable for accurate and direct comparison as the MW dependence on polymer properties is minimal.

In addition, polymer thermal stability was evaluated by TGA under a N_2 atmosphere (Figure S1). All C_{16}CPDT series polymers showed high temperature decomposition temperatures (determined as 5% loss on weight), in all cases over 410 °C (Table 1). DSC scans were performed, showing two thermal transitions which are common for C_{16}CPDT based polymers: (i) a melting endotherm at ~15 °C and (ii) corresponding crystallization at ~0 °C on the heating and cooling scans, respectively (Figure 2). Those thermal transitions, which are
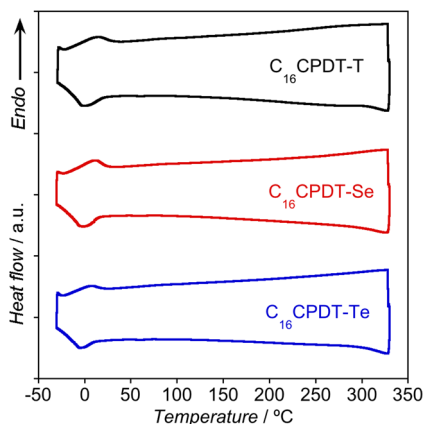

Figure 2. DSC traces for C_{16}CPDT based polymers acquired at 10 °C/min under N_2.

reproducible by heating and cooling several times, are associated with the linear alkyl chain melting and crystallization. This suggests some order on the polymer microstructure through the alkyl chains.

3.2. Optical Properties. The effect on the heteroatom on the polymer electronic properties was investigated. UV−vis absorption spectra were acquired in both solution and solid

state, showing a pronounced shift not only on λ_{max} and λ_{onset} but also on the absorption spectral shape depending on the chalcogen atom (Figure 3a). Optical data can be found in Table 2.

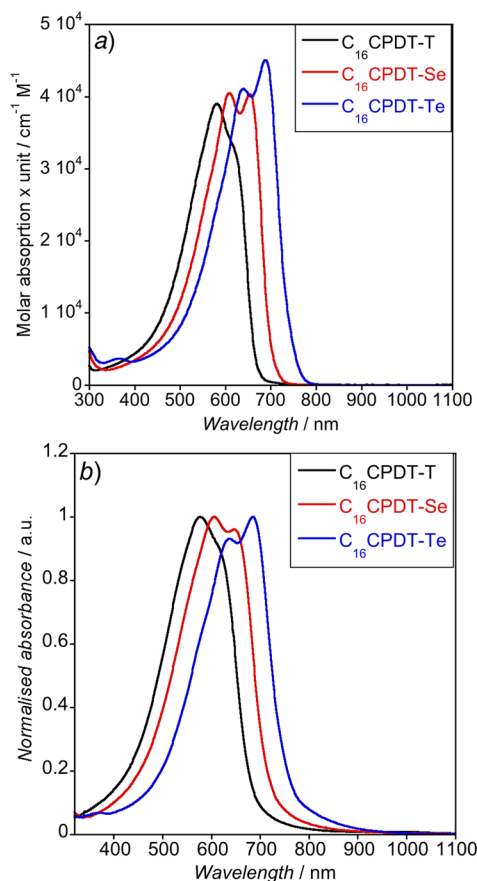**Figure 3.** UV−vis absorption spectra of C_{16}CPDT based polymers in (a) chlorobenzene solution and (b) thin film.

Table 2. Optical Properties of C_{16}CPDT Based Polymers in Solution and Solid State

	solution (PhCl)		film		
polymer	λ_{max}^a (nm)	λ_{onset} (nm)	λ_{max}^a (nm)	λ_{onset} (nm)	E_{gap}^b (eV)
C_{16}CPDT-T	578 (613)	667	576 (617)	684	1.81
C_{16}CPDT-Se	609 (653)	702	606 (652)	720	1.72
C_{16}CPDT-Te	638 (689)	744	634 (684)	757	1.64

[a]Values in parentheses correspond to the low-energy or aggregated polymer band. [b]Optical gap from the onset of absorption spectrum.

In addition, absorption maxima and electronic transition profiles in solid-state films (Figure 3b) are very close to the solution measurements, with a maximum shift of only 5 nm. This suggests that a minimal chain order increment takes place in the solid state.

A clear trend was observed on the optical gap between polymers. C_{16}CPDT-T (1.81 eV) exhibited the widest gap, followed by C_{16}CPDT-Se (1.72 eV) and C_{16}CPDT-Te (1.64 eV) which had the narrowest gap. This trend can be explained in terms of how aromaticity is reduced when bigger heteroatoms are used. Larger chalcogen atoms in conjugated five-member rings, despite being easier to polarize, exhibit a
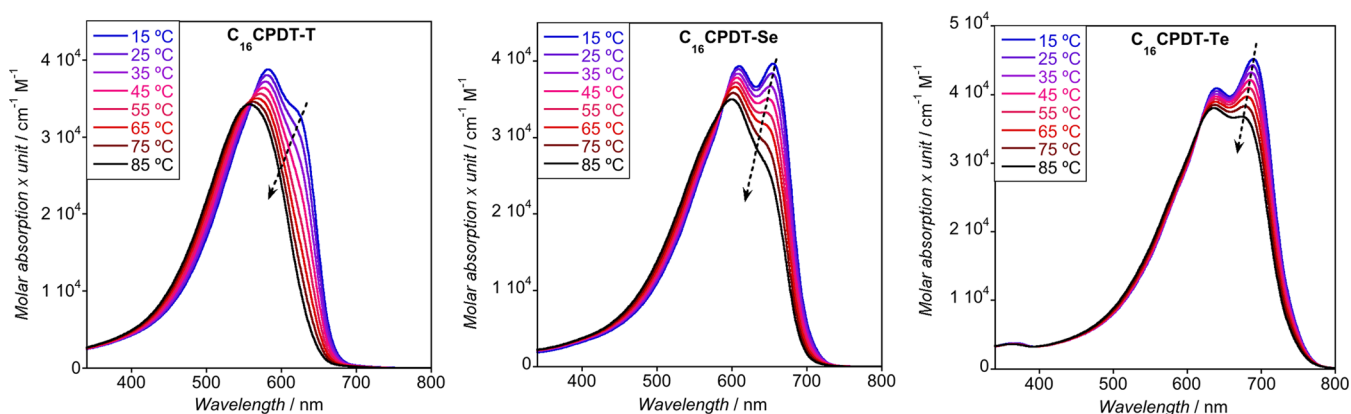
Figure 4. Temperature-dependent UV–vis absorption for C_{16}CPDT-T (left), C_{16}CPDT-Se (middle), and C_{16}CPDT-Te (right) polymers in chlorobenzene solution. Arrows indicate the trend upon heating.

poor overlap with diene carbon p_z orbitals due to the larger size, and thus its aromaticity is reduced following Te < Se < S.[11] Computed neat chalcogenophene bonds and angles (Table S1) showed a larger distance C_α-heteroatom together with a decrease in heteroatom bonding angle as the chalcogen size increases. This altered heterocycle geometry confirms the poor orbital overlap obtained for larger chalcogenophenes. In addition to that, the bond distance $C_\alpha-C_\beta$ is reduced while $C_\beta-C_{\beta'}$ is enlarged, confirming an enhanced diene character for larger chalcogen heterocycles and therefore a lost on ring aromaticity. Hence, this aromaticity lost will lead to a HOMO destabilization (i.e., upward shift) together with a LUMO stabilization (i.e., downward shift) and narrowing the band gap, which is in a good agreement with our findings.

All three C_{16}CPDT polymers showed a dual band absorption profile. The high-energy band is attributed to the non-aggregated polymer electronic transition while the low-energy band is assigned to the aggregated polymer absorption. In this case, we observed that red-shifted band contribution is more pronounced as the chalcogen atom size increases. This is due to the stronger intermolecular interactions between chalcogen atoms following Te > Se > S.[14,37] In order to further confirm that is that the red-shifted band corresponds to the aggregated polymer, temperature-dependent UV–vis experiments were carried out in solution (Figure 4).

As can be seen, the low-energy band disappears completely upon heating for C_{16}CPDT-T, showing only one Gaussian shaped band corresponding to nonaggregated polymer. For C_{16}CPDT-Se, the low-energy band almost completely disappears upon heating, while for C_{16}CPDT-Te it decreased only slightly. In addition, an isosbestic point can be observed, indicating a clean and reversible conversion. Those observations suggest that stronger Te–Te interactions exist, forcing the C_{16}CPDT-Te polymer to be in its aggregated state even at high temperature.

3.3. Electrochemical Properties. Having studied the heavy atom effect on the optical gap, we performed electrochemical measurements on spin-coated films in order to determine effect on the specific frontier energy levels. Cyclic voltammetry (CV) experiments were performed, and the results for the second scan are shown in Figure 5. We observed two different profiles: (i) a reversible oxidation peak at ~0.8 V vs Ag/AgCl, which is very similar for all three polymers, and (ii) shoulder arising at ~0.5 V vs Ag/AgCl, the intensity of which is directly related to the chalcogen atom size.
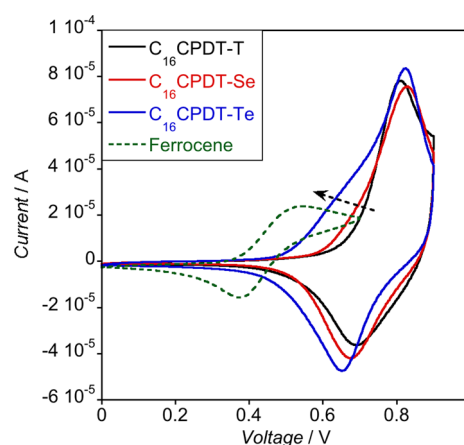

Figure 5. Cyclic voltammetry traces of C_{16}CPDT based polymers and ferrocene acquired in 0.1 M [TBA][PF$_6$] acetonitrile solution at 50 mV/s.

The former reversible process can be related to the oxidation and subsequent reduction of nonaggregated polymers chains. We speculate that the latter oxidation process, the irreversible shoulder, could be related to the aggregated polymer oxidation. As discussed previously in the optical section, increasing the size of the chalcogen atoms strengthens the intermolecular heteroatom–heteroatom interactions and therefore enhances the presence of aggregation. Polymer aggregation not only narrows the optical gap but also raises the HOMO energy level, giving an irreversible shoulder on the CV scans.

3.4. Computational Properties and Energy Levels. In order to further understand the optical and electrochemical trends observed for the polymer series, we performed hybrid DFT calculations on trimeric systems in vacuum at the B3LYP/ 6-311G(d) level of theory (Figure 6). In this case, Stuttgart–Dresden (SDD) effective core potentials (ECP) were used to describe the heavy atoms selenium and tellurium. For all the polymer series, the HOMO has a π character, and it is delocalized over the CPDT and chalcogenophene units, with minimal presence on the chalcogen atom. This led to a minimal shift on the HOMO energy level among samples, and it can be experimentally observed in the reversible peak on the electrochemical measurements (Figure 5), where a minimal difference is observed. It is worth emphasizing that the simulations are performed for isolated trimeric systems in the gas phase, and therefore they were unable to reproduce the
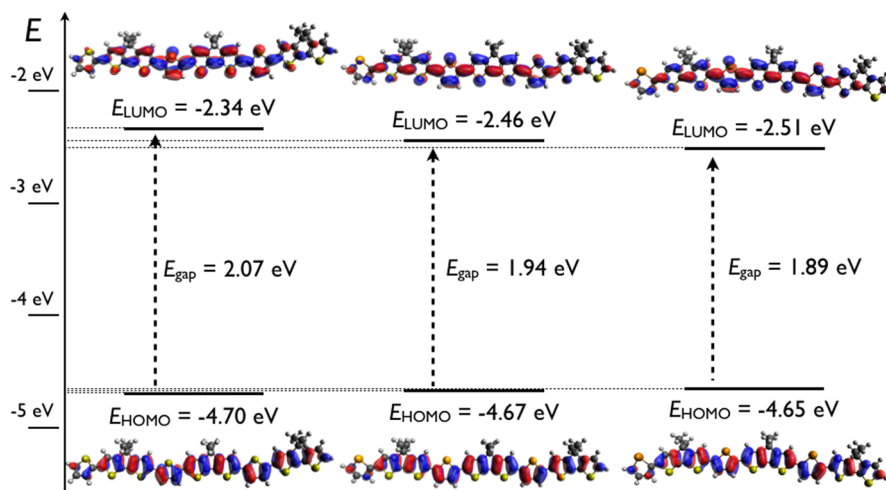
Figure 6. Molecular orbital distribution of HOMO (bottom) and LUMO (top) for C_{16}CPDT-T (left), C_{16}CPDT-T (middle), and C_{16}CPDT-Te (right) at the B3LYP/6-311G(d) level of theory (isodensity = 0.02) and SDD ECP for Se and Te atoms. The absolute values of E_{HOMO}, E_{LUMO}, and E_{gap} shown are obtained by computational means.

observed aggregation effects (i.e., CV irreversible oxidation shoulder), as they could not take in account any intermolecular interactions.

On the other hand, the LUMO has a strong π^* character with electron density fully delocalized over CPDT and chalcogenophene unit, but it is also delocalized over the heteroatom. This led to a noticeable deeper shift on the LUMO energy level upon increasing the heteroatom size, and it is mainly responsible for narrowing the band gap on our C_{16}CPDT polymer series.

Interestingly, tellurophene itself has a σ based HOMO and σ^* LUMO, in contrast to thiophene and selenophene where the HOMO and LUMO are π and π^* based, respectively (Figure S2).[12] This explains the different chemical reactivity, for example, the preference for direct bromination of tellurium atom rather ring's α-bromination.[14] However, once incorporated into the polymer system, tellurium HOMO−1 and LUMO+1 (i.e., π and π^* based orbitals, respectively) hybridize with the CPDT π orbitals, resulting in a polymer system with marked π and π^* character for HOMO and LUMO, respectively.

Time-dependent (TD) DFT calculations were also performed in order to simulate the UV−vis spectra (Figure S3). Not unexpectedly, the main electronic transition is HOMO to LUMO ($\pi-\pi^*$), therefore verifying a decrease in the band gap upon increase of chalcogen atom size. Interestingly, the oscillator strength for the main electronic transition increased with the chalcogen atom size, confirming the higher molar absorption coefficient obtained for polymers containing larger chalcogenophenes (Table S2). As discussed before, the dual band observed in the UV−vis spectra cannot be effectively reproduced by TD-DFT as the calculations did take into account aggregation effects.

4. CONCLUSIONS

In summary, we have designed and synthesized three conjugated polymers containing a common C_{16}CPDT unit with thiophene, selenophene, and tellurophene comonomers. Molecular weights and polydispersity obtained for the polymer series are very similar, thus ensuring an accurate comparison between samples. Thermal stability and thermal transitions determined by DSC were not influenced by the nature of the

chalcogenophene heteroatom. On the other hand, optical properties are noticeably different. The increasing heteroatom size (S < Se < Te) had two main effects: (i) a red-shifted absorption of ∼35 nm by narrowing the band gap, mainly due to a decrease of chalcogenophene aromatic character, and (ii) an increase on polymer aggregates due to stronger intermolecular heteroatom−heteroatom interaction for larger and heavier chalcogen atoms. The latter effect can be also observed on the electrochemical traces, resulting in prompt oxidation shoulder and therefore a rise in the HOMO energy level.

It is important to additionally recognize that solubility issues could arise due to presence of aggregates. This is particularly significant for tellurophene as a result of the stronger Te−Te interactions. One way to overcome this problem is increasing the alkyl chain length (i.e., solubilizing strength) although polymer systems of comparable molecular weights containing thiophene equivalent demonstrated good solubility.

■ ASSOCIATED CONTENT

Ⓢ Supporting Information

Thermogravimetric analysis, additional DFT and TD-DFT calculations, and full ref 27. This material is available free of charge via the Internet at http://pubs.acs.org.

■ AUTHOR INFORMATION

Corresponding Author

*E-mail m.planells@imperial.ac.uk (M.P.).

Notes

The authors declare no competing financial interest.

■ ACKNOWLEDGMENTS

■ REFERENCES

(1) Heeger, A. J. *Adv. Mater.* **2014**, *26*, 10.

(2) Dou, L.; You, J.; Hong, Z.; Xu, Z.; Li, G.; Street, R. A.; Yang, Y. *Adv. Mater.* **2013**, *25*, 6642.

(3) Kuik, M.; Wetzelaer, G. J.; Nicolai, H. T.; Craciun, N. I.; De Leeuw, D. M.; Blom, P. W. *Adv. Mater.* **2014**, *26*, 512.

(4) Sirringhaus, H. *Adv. Mater.* **2014**, *26*, 1319.

(5) Dong, H.; Fu, X.; Liu, J.; Wang, Z.; Hu, W. *Adv. Mater.* **2013**, *25*, 6158.

(6) Rivnay, J.; Owens, R. M.; Malliaras, G. G. *Chem. Mater.* **2014**, *26*, 679.

(7) Adhikari, B.; Majumdar, S. *Prog. Polym. Sci.* **2004**, *29*, 699.

(8) Li, Z.; Li, Q.; Qin, J. *Polym. Chem.* **2011**, *2*, 2723.

(9) Sun, D.; Ehrenfreund, E.; Valy Vardeny, Z. *Chem. Commun.* **2014**, *50*, 1781.

(10) Schroeder, B. C.; Ashraf, R. S.; Thomas, S.; White, A. J. P.; Biniek, L.; Nielsen, C. B.; Zhang, W.; Huang, Z.; Tuladhar, P. S.; Watkins, S. E.; Anthopoulos, T. D.; Durrant, J. R.; McCulloch, I. *Chem. Commun.* **2012**, *48*, 7699.

(11) Otsubo, T.; Takimiya, K. In *Handbook of Thiophene-Based Materials*; John Wiley & Sons, Ltd.: New York, 2009; p 321.

(12) Modelli, A.; Guerra, M.; Jones, D.; Distefano, G.; Irgolic, K. J.; French, K.; Pappalardo, G. C. *Chem. Phys.* **1984**, *88*, 455.

(13) McCormick, T. M.; Carrera, E. I.; Schon, T. B.; Seferos, D. S. *Chem. Commun.* **2013**, *49*, 11182.

(14) McCormick, T. M.; Jahnke, A. A.; Lough, A. J.; Seferos, D. S. *J. Am. Chem. Soc.* **2012**, *134*, 3542.

(15) Kaur, M.; Yang da, S.; Shin, J.; Lee, T. W.; Choi, K.; Cho, M. J.; Choi, D. H. *Chem. Commun.* **2013**, *49*, 5495.

(16) Jahnke, A. A.; Howe, G. W.; Seferos, D. S. *Angew. Chem., Int. Ed.* **2010**, *49*, 10140.

(17) Jahnke, A. A.; Djukic, B.; McCormick, T. M.; Buchaca Domingo, E.; Hellmann, C.; Lee, Y.; Seferos, D. S. *J. Am. Chem. Soc.* **2013**, *135*, 951.

(18) He, G.; Kang, L.; Torres Delgado, W.; Shynkaruk, O.; Ferguson, M. J.; McDonald, R.; Rivard, E. *J. Am. Chem. Soc.* **2013**, *135*, 5360.

(19) Patra, A.; Wijsboom, Y. H.; Leitus, G.; Bendikov, M. *Chem. Mater.* **2011**, *23*, 896.

(20) Lee, S. K.; Cho, N. S.; Cho, S.; Moon, S.-J.; Lee, J. K.; Bazan, G. C. *J. Polym. Sci., Part A: Polym. Chem.* **2009**, *47*, 6873.

(21) Detty, M. R.; O'Regan, M. B. In *Chemistry of Heterocyclic Compounds*; John Wiley & Sons, Inc.: New York, 2008; p 363.

(22) Awschalom, D. D.; Flatte, M. E. *Nat. Phys.* **2007**, *3*, 153.

(23) Mishra, A.; Ma, C.-Q.; Segura, J. L.; Bäuerle, P. In *Handbook of Thiophene-Based Materials*; John Wiley & Sons, Ltd.: New York, 2009; p 1.

(24) Al-Hashimi, M.; Labram, J. G.; Watkins, S.; Motevalli, M.; Anthopoulos, T. D.; Heeney, M. *Org. Lett.* **2010**, *12*, 5478.

(25) Shahid, M.; McCarthy-Ward, T.; Labram, J.; Rossbauer, S.; Domingo, E. B.; Watkins, S. E.; Stingelin, N.; Anthopoulos, T. D.; Heeney, M. *Chem. Sci.* **2012**, *3*, 181.

(26) Sweat, D. P.; Stephens, C. E. *Synthesis* **2009**, *2009*, 3214.

(27) Frisch, M. J.; et al. *Gaussian 09, Revision B.01*; Gaussian Inc.: Wallingford, CT, 2009.

(28) Andrae, D.; Häußermann, U.; Dolg, M.; Stoll, H.; Preuß, H. *Theor. Chim. Acta* **1990**, *77*, 123.

(29) Hanwell, M.; Curtis, D.; Lonie, D.; Vandermeersch, T.; Zurek, E.; Hutchison, G. *J. Cheminf.* **2012**, *4*, 17.

(30) Bauernschmitt, R.; Ahlrichs, R. *Chem. Phys. Lett.* **1996**, *256*, 454.

(31) Tozer, D. J.; Handy, N. C. *J. Chem. Phys.* **1998**, *109*, 10180.

(32) O'Boyle, N. M.; Tenderholt, A. L.; Langner, K. M. *J. Comput. Chem.* **2008**, *29*, 839.

(33) Coppo, P.; Cupertino, D. C.; Yeates, S. G.; Turner, M. L. *Macromolecules* **2003**, *36*, 2705.

(34) Bronstein, H.; Leem, D. S.; Hamilton, R.; Woebkenberg, P.; King, S.; Zhang, W.; Ashraf, R. S.; Heeney, M.; Anthopoulos, T. D.; Mello, J. D.; McCulloch, I. *Macromolecules* **2011**, *44*, 6649.

(35) Ashraf, R. S.; Schroeder, B. C.; Bronstein, H. A.; Huang, Z.; Thomas, S.; Kline, R. J.; Brabec, C. J.; Rannou, P.; Anthopoulos, T. D.; Durrant, J. R.; McCulloch, I. *Adv. Mater.* **2013**, *25*, 2029.

(36) Li, W.; Yang, L.; Tumbleston, J. R.; Yan, L.; Ade, H.; You, W. *Adv. Mater.* **2014**, *26*, 4456.

(37) Wudl, F.; Aharon-Shalom, E. *J. Am. Chem. Soc.* **1982**, *104*, 1154.